

# In vitro Anti SARS-CoV-2 Activity and Docking Analysis of *Pleurotus ostreatus*, *Lentinula edodes* and *Agaricus bisporus* Edible Mushrooms

Shaza M Elhusseiny<sup>1</sup>, Taghrid S El-Mahdy<sup>2</sup>, Nooran S Elleboudy<sup>3</sup>, Ibrahim S Yahia<sup>4,5</sup>, Mohamed MS Farag<sup>6,7</sup>, Nasser SM Ismail<sup>8</sup>, Mahmoud A Yassien<sup>3</sup>, Khaled M Aboshanab<sup>3</sup>

<sup>1</sup>Department of Microbiology and Immunology, Faculty of Pharmacy, Ahrm Canadian University (ACU), Cairo, 12566, Egypt; <sup>2</sup>Department of Microbiology and Immunology, Faculty of Pharmacy, Helwan University, Cairo, Egypt; <sup>3</sup>Department of Microbiology and Immunology, Faculty of Pharmacy, Ain Shams University, Cairo, 11566, Egypt; <sup>4</sup>Laboratory of Nano-Smart Materials for Science and Technology (LNSMST), Department of Physics, Faculty of Science, Research Center for Advanced Materials Science (RCAMS), King Khalid University, Abha, Saudi Arabia; <sup>5</sup>Nanoscience Laboratory for Environmental and Bio-Medical Applications (NLEBA), Semiconductor Lab, Metallurgical Lab, Physics Department, Faculty of Education, Ain Shams University, Cairo, Egypt; <sup>6</sup>Botany and Microbiology Department, Faculty of Science, Al-Azhar University, Cairo, 11884, Egypt; <sup>7</sup>Armed Forces College of Medicine (AFCM), Cairo, Egypt; <sup>8</sup>Department of Pharmaceutical Chemistry, Faculty of Pharmacy, Future University in Egypt, Cairo, 11835, Egypt

Correspondence: Khaled M Aboshanab, Department of Microbiology and Immunology, Faculty of Pharmacy, Ain Shams University, Organization of African Unity Street, Abbassia, Cairo, 11566, Egypt, Tel +20 1-0075-82620, Fax +20 224051107, Email aboshanab2012@pharma.asu.edu.eg

**Background:** Fungi are rich source of biologically active metabolites aimed for the improvement of human health through the prevention of various diseases, including infections and inflammatory disorders.

**Aim:** We aimed to in vitro examine the anti-SARS CoV-2 activity of the aqueous extract of each *Pleurotus (P.) ostreatus*, *Lentinula (L.) edodes* and *Agaricus (A.) bisporus* edible mushroom followed by docking analysis of certain metabolites against the severe acute respiratory syndrome coronavirus 2 (SARS-CoV-2)-main protease (protease M<sup>Pro</sup>).

**Methods:** Antiviral and cytotoxic effects were tested on hCoV-19/Egypt/NRC-3/2020/Vero-E6 cells and analyzed via (3-(4,5-dimethylthiazol-2-yl)-2,5-diphenyltetrazolium bromide Assay (MTT) assay. Ligand-protein and protein-protein docking studies were performed to explore the interaction of different mushroom extracts at the binding site of protease M<sup>Pro</sup>. Molecular dynamics (MD) simulations were performed on the most promising ligand-target complexes to investigate their dynamic properties and confirm docking results.

**Results:** Substantial antiviral activities with an IC<sub>50</sub> of 39.19, 26.17, and 10.3.3 µg/mL and a selectivity index (SI) of 4.34, 3.44, and 1.5 for *P. ostreatus*, *L. edodes* and *A. bisporus*, were observed, respectively. Docking analysis revealed that, catechin from three mushroom isolates, chlorogenic acid from *A. bisporus*, kamperferol of *P. ostreatus* and quercetin from *L. edodes*, with a C-DOCKER interaction energy in the range of 22.8–37.61 (Kcal/mol) with protease compared to boceprevir ligand of 41.6 (Kcal/mol). Docking of superoxide dismutase, catalase from the three mushrooms, tyrosinase from *A. bisporus* showed ligand contact surface area with the protein as 252.74 Å<sup>2</sup> while receptor contact surface area was 267.23 Å<sup>2</sup>.

**Conclusion:** *P. ostreatus*, *L. edodes* and *A. bisporus* have potential and remarkable in vitro antiviral activities against SARS-CoV-2. Quercetin from *L. edodes*, Kaempferol from *P. ostreatus*, chlorogenic acid and ascorbic acid, catechin, superoxide dismutase and catalase of the three mushrooms extracts were effectively bounded to M<sup>Pro</sup> of SARS-CoV-2 as conferred by docking analysis.

**Keywords:** edible mushrooms, *Pleurotus ostreatus*, *Lentinula edodes*, *Agaricus bisporus*, SARS-CoV-2, cytotoxicity

## Introduction

Coronaviruses are single-strand RNA viruses that can spread between humans and animals, and they have been linked to a variety of infections.<sup>1</sup> These infections can manifest as symptoms ranging from a simple cold to far more serious illnesses and complications.<sup>1</sup> The Severe Acute Respiratory Syndrome (SARS-CoV, or SARS) and the Middle East

Respiratory Syndrome (MERs-CoV, or MERs) are the highly pathogenic and have resulted in regional and pandemic outbreaks.<sup>2,3</sup>

Regardless, the fact that a lot of effort is being put towards vaccine development and drug repurposing, the majority of the pharmaceuticals used to treat COVID-19 symptoms are based mainly on clinical symptoms.<sup>4</sup> Many efforts have been conducted for testing various natural products for their potential anti SARS-CoV-2 activities.<sup>5</sup> To avert SARS-CoV-2 infection, many agents are being investigated in laboratory or clinical studies.<sup>6</sup> However, with these drugs, there is constantly high probability of drug non-susceptibility, particularly with viral enzyme inhibitors.<sup>7</sup> Accordingly, there is a strong demand to develop and explore novel and economic antiviral agents.<sup>8</sup> Apart from their nutritional properties, mushrooms are rich in biologically active components that exhibit merit of pharmacological actions.<sup>9</sup> Mushrooms represent an important source of natural products with high medical relevance. Polyphenols, as flavonoids, are widespread compounds in the plant kingdom. In this study, the genus *Pleurotus*, *Lentinula* and *Agaricus* are a common member of Basidiomycete family, which is made up of versatile group of mushrooms that are valued for their nutritious and health benefits.<sup>10,11</sup> These mushroom species (known as edible mushrooms) are cholesterol free, low-fat and low sodium food products.<sup>12</sup> Besides, they are valued for their vital source of water- and fat-soluble vitamins, chitin, minerals, glucans, and proteins. Also, such mushrooms contain crucial compounds with biological activity such as phenolic acids, ergosterol, antioxidant amino acid and lovastatin.<sup>13</sup> Accordingly, the fruiting bodies and mycelia of *Pleurotus* species possess various therapeutic activities, such as antioxidant, anti-inflammatory, antimicrobial, antitumor and immune-regulating activities.<sup>14,15</sup> Pleuran polysaccharide is used as a food supplement to enhance immunity among infants and adults.<sup>16</sup> The structural characterization of lentinan (LNT-1) was determined from *L. edodes* mycelia (shiitake).<sup>16</sup> Besides, LNT-1 proved to regulate the innate immune response and possess antiviral activity. The natural immunity is a vital factor for controlling the severity and prognosis of COVID-19 cases.<sup>16,17</sup> Moreover, the *L. edodes*, *P. ostreatus* and *A. bisporus* mushrooms are some of the major dietary suppliers of Beta-glucans ( $\beta$ -glucans).<sup>18</sup>  $\beta$ -glucans, naturally occurring polysaccharides, are present as constituents of the cell wall of cereal grains, mushrooms, algae, or microbes including bacteria, fungi, and yeast.  $\beta$ -glucans has important role on the immune system relative to cancer treatment, infection immunity, and restoration of damaged bone marrow. McCarty and DiNicolantonio recently described the potential role of  $\beta$ -glucan for enhancing type 1 interferon activity against influenza and coronavirus.<sup>19</sup> As an immunomodulating agent,  $\beta$ -glucan acts through the activation of innate immune cells such as macrophages, dendritic cells, granulocytes, and natural killer cells; resulting in  $\beta$ -glucan exert multiple effects against various ailments. In a previous research conducted in our Lab, the phenolic, flavonoid and vitamin contents followed by untargeted LC/MS- TripleTOF based proteomics analysis of *L. edodes*, *P. ostreatus* and *A. bisporus* mushrooms were carried out.<sup>20</sup> This analysis led to identification and characterization of quercetin, kaempferol, apigenin, ascorbic acid and catechin which are vital bioactive compounds. Accordingly, in this study we aimed to in vitro investigate the anti SARS CoV-2 activities of *P. ostreatus*, *L. edodes* and *A. bisporus* mushroom extracts and test its anti-viral potential followed by docking studies of certain abundant small and macromolecules against SARS-CoV-2 protease (protease M<sup>Pro</sup>), the main enzyme involved in the viral replication.

## Materials and Methods

### Mushroom Materials

The fruiting bodies of the strain *P. ostreatus*, *L. edodes* and *A. bisporus* were collected from the Orman botanical garden, Cairo, Egypt. Identification was done through sequencing of the internal transcribed (ITS) region of the ribosomal DNA in our previous study with accession number MK603976, MN622787 and MZ642282, respectively.<sup>20</sup> The phylogenetic analysis was carried out as previously reported.<sup>21</sup> The mushroom fruiting bodies (500 g) were air dried and powdered and stored in aerated area at room temperature until further use. For mycelia isolation, sterile surgical blades were used to cut the fruit to expose the inner mycelia, the mycelia were then inoculated on sterile Rose Bengal Chloramphenicol agar (RBA; Sigma-Aldrich, Milan, Italy) plates and incubated at 25 °C for 7 days. The mycelia were then sub-cultured on sterile Potato Dextrose agar (PDA; Merck, Darmstadt, Germany) media every month for preservation.<sup>22</sup>

## Preparation of Aqueous Extracts

Aliquots (500 g) of each of the powdered mushroom isolates were macerated in distilled water for three successive days at room temperature, ultra-sonicated for one hour then filtered. Ethanol (80%) was used for yield preservation and before use a rotary evaporator was exploited to evaporate ethanol at a water bath below 50 °C. *P. ostreatus*, *L. edodes* and *A. bisporus* aqueous extract (500 mL) was freeze dried to yield dry extract (20 g).<sup>23</sup>

## Phenolic and Flavonoid Determination

High performance liquid chromatography (HPLC) Analysis was carried out for the identification and quantification of selected phenolic and flavonoid compounds according to the method of Singh et al.<sup>24</sup> In a previous research conducted in our Lab, the phenolic and flavonoid including, catechin was found in all three mushroom extracts (retention time 26.48 min), chlorogenic acid was detected in *A. bisporus* extract at retention time 29.61 min, and quercetin was found in *L. edodes* extract at retention time 56.86 min. Kaempferol and apigenin were only detected in *P. ostreatus* at 59.13 and 59.56 min, respectively.<sup>20</sup> These results were confirmed by including a mixture of standard phenolic and flavonoid that has shown the same retention times as those of the detected in the mushroom extract.<sup>20</sup>

## Vitamin Analysis

Identification and quantification the water-soluble vitamins and fat-soluble vitamin content of the mushroom extract was done according to Duffy et al.<sup>25</sup> Water- and fat-soluble vitamin contents were detected via HPLC.<sup>20</sup> Mushroom species are rich in vitamin C, riboflavin was only observed in *A. bisporus*. Vitamin D was encountered in the three mushroom species. Determined amounts of vitamins B3, B6 were noticed.<sup>20</sup>

## Untargeted LC/MS – Triple TOF-Based Proteomics Analysis

Analysis of proteomics was handled in the proteomics and metabolomics unit at Children's Cancer Hospital 57357, Cairo, Egypt. Protein extraction and denaturation of *P. ostreatus*, *L. edodes* and *A. bisporus* samples were done as previously reported.<sup>20</sup> Analysis of Proteome was conducted using LC-Triple TOF-MS analysis with a "95% confidence of identification" and a false discovery rate (FDR) of < 5% and. *P. ostreatus*, a total of 753 proteins were identified. A total of 433 proteins were detected in *L. edodes* and a total of 489 proteins in *A. bisporus*. The MS-Triple TOF data were analyzed by ProteinPilot with the Paragon Algorithm and the spectrum of the mushroom extract analyzed by Analyst TF 1.7.1 (Sciex software) as previously conducted in our Lab.<sup>20</sup>

## Anti SARS CoV-2 Assay

### Virus and Cell Culture

hCoV-19/Egypt/NRC-3/2020 (Accession Number on GSAID: EPI\_ISL\_430820) and Vero-E6 cells were obtained from Nawah Scientific, Cairo, Egypt. Vero-E6 cells were maintained on Dulbecco's Modified Eagle's medium (DMEM) containing Fetal Bovine Serum (FBS; 10%) (Invitrogen, Germany) and Penicillin/Streptomycin (1% pen/strep) antibiotic mixture, at 37 °C, 5% CO<sub>2</sub> to generate monolayers 24 hours prior to infection.<sup>26</sup>

### Propagation of the SARS-CoV-2 Virus

One day before infection, Vero cells were seeded in cell culture flasks. Infection was done at a multiplicity of infection (MOI) and propagation was performed as previously reported.<sup>26</sup> The supernatants were gathered and centrifuged at 2500 rpm for 5 min for small particulate cell debris removal.

### MTT (3-(4, 5-Dimethylthiazol-2-Yl)-2, 5-Diphenyltetrazolium Bromide Assay

The cytotoxic activity of the extracts was tested on VERO-E6 cells by using the MTT method with minor modifications. Briefly, in 96 well-plates, the cells were seeded (100 µL/well at a density of 3×10<sup>5</sup> cells/mL) and incubated in 5% CO<sub>2</sub> for 24 hours at 37 °C. After 24 hours, cells were treated with the tested extract at various concentrations in triplicates (1000, 500, 250, 125, 62.5, 31.25, 15.62, 7.81, 3.90 and 1.95 µg/mL). The supernatants were discarded 24 hours later, and the cytotoxicity was calculated as previously reported.<sup>26</sup>

### Determination of Inhibitory Concentration 50 (IC<sub>50</sub>)

A  $2.4 \times 10^4$  Vero-E6 cells inoculum, in 96-well tissue culture plates were distributed in each well and incubated at 37 °C overnight under 5% CO<sub>2</sub> condition. The cell monolayers were washed and exposed to virus adsorption (hCoV-19/Egypt/NRC-03/2020) for 60 min at room temperature. The cell monolayers were overlaid with DMEM (100 µL) including various concentrations (1000, 500, 250, 125, 62.5, 31.25, 15.62, 7.81, 3.90 and 1.95 µg/mL) of the extract. The Inhibitory concentration 50 (IC<sub>50</sub>) and Selectivity index (SI) were calculated as previously determined.<sup>26</sup>

### Molecular Docking Analysis

Molecular docking is an essential tool in drug design and discovery used to identify interactions between the key amino acids of the target protein and different ligands.<sup>27,28</sup> Hereby, in this study, Discovery Studio 4.0 Software (Waltham, MA, USA); [<https://discover.3ds.com/discovery-studio-visualizer-download.com>] was used to perform molecular docking simulations to estimate the binding affinity of different ligands of either small molecules or macromolecules interacting with the identified receptor. The crystal structure of SARS-CoV-2 main protease M<sup>Pro</sup> in complex with boceprevir (PDB ID: 6XQU) was downloaded from Protein Data Bank ([www.rcsb.org](http://www.rcsb.org)). Target Protein was cleaned and hydrogen atoms was added to amino acid residues, to complete the missing residues. Also, water molecules was removed, and Force Field using CHARMM and MMFF94 partial charge was applied. Protease protein was prepared and minimized. The active site was defined and Boceprevir ligand was removed to be ready for docking with the new ligands.

### Molecular Docking of Small Molecules

Small molecule ligands were prepared for molecular modeling simulation study where docking of kaempferol, quercetin, ascorbic acid, catechin and caffeic acid into the binding site of protease using C-DOCKER algorithm was performed in addition to Boceprevir ligand docking. The new ligands were previously prepared via “Prepare Ligand” protocol. Force Field using CHARMM and MMFF94 partial charge was applied. The resulted binding modes compared to that of Boceprevir ligand was studied to determine the biological activity and to analyze the binding affinity to the target.

### Molecular Docking of Macromolecules

The Crystal Structure of Agaricus Bisporus Mushroom Tyrosinase (PDB ID: 2Y9X), ubiquitin-like protein, Rub1 (PDB ID: 1BT0), Human Nuclear Valosin containing protein Like (NVL), C-terminal AAA- ATPase domain (PDB ID: 2X8A), Human Erythrocyte Catalase Cyanide Complex (PDB ID: 1DGG), Estrogen Sulfotransferase With Inactive Cofactor Pap And Vanadate (PDB ID: 1BO6) were all downloaded from protein data bank and prepared for docking. Where clean protein was applied followed by simulation with CHARMM forcefield and MMFF94 partial charge. Preparation of protein was performed via prepare protein for ligand proteins before docking and co-crystallized ligands were removed. ZDOCK algorithm was applied on the prepared SARS-CoV-2 main protease (PDB ID: 6XQU), the Angular Step Size was set at 6 for finer conformational sampling to produce more accurate predictions. Rerank initial-stage ZDOCK predictions with detailed electrostatics, Van der Waals, and desolvation energy terms (ZRANK) was set true, number of top scoring poses to be rescored with the ZRANK algorithm was set to be 20 and finally number of top-scoring poses to cluster was set at 20.

### Molecular Dynamics Simulation

Molecular Dynamics Simulation (MD simulation) is considered a valuable approach to validate the stability of the docked ligands.<sup>29</sup> The study provides information about the dynamic behavior of both the ligand and the target protein and evaluate the ligand’s key binding interactions within the docked complex.<sup>29</sup> Hereby, the ligand-protein and protein-protein complexes showing the most promising molecular docking results, were selected and enrolled within 100 ns all-atom MD simulation using Discovery Studio 4.0. CHARMM force field parameters for the investigated ligands was generated automatically. Each ligand protein complex was solvated allowing about 10 Å marginal distance. Protein residues were first adjusted to standard ionization states at normal physiological conditions (pH 7.0), and the selected complexes were then neutralized. Finally, the MD simulations were run for 100 ns under constant pressure (NPT

ensemble). Data calculation including calculation of the binding free energy, root-mean-square deviation (RMSD) and root-mean-square fluctuation (RMSF) in order to investigate the possible interactions of ligands with the important protein residues and to predict stability of the docked complexes at the binding site.<sup>29</sup>

## Statistical Analysis

All experiments were conducted in triplicates. Statistical tests and graphical data presentation were performed using GraphPad Prism 5.01 software.

## Results

### Molecular Identification of the Mushroom Strain

Alignment of partial ITS spacers 1 (ITS1) and ITS spacers 4 (ITS4) ribosomal RNA gene sequence with standard reference taxa in the Blast GenBank® database with highest percentage of identity resulted in identification of the mushroom species as *P. ostreatus*, *L. edodes* and *A. bisporus* with accession number MK603976, MN622787 and MZ642282, respectively. The phylogenetic trees of the respected three mushrooms are displayed in [Figures S1–S3 \(Supplementary Materials\)](#).

### Anti-SARS-CoV-2 Activities

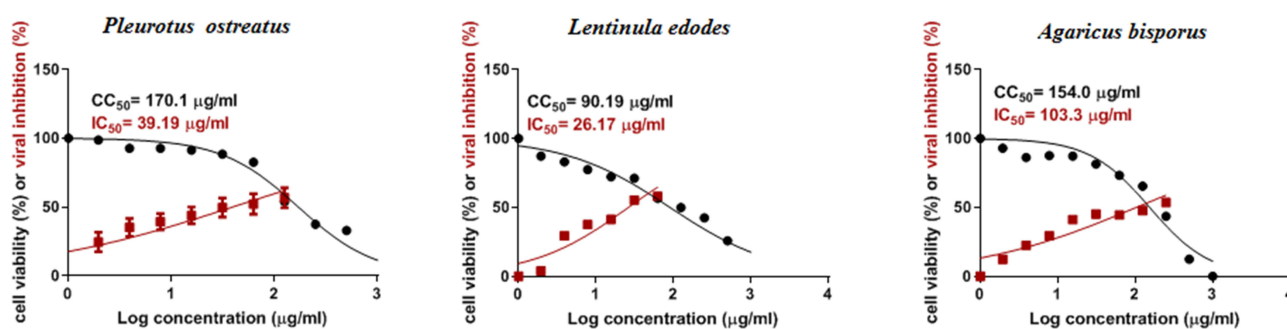
The antiviral screening revealed that, the tested mushroom samples exhibited a promising in vitro activity against SARS-CoV-2 and has declared antiviral activities with a high SI as 4.34 and 3.44 for *P. ostreatus* and *L. edodes* while low SI of 1.5 was observed with *A. bisporus* for antiviral activity relative to cellular toxicity. [Figure 1](#), the recorded half cytotoxic concentration (CC<sub>50</sub>) was 170.1, 90.19 and 154 µg/mL, while the half inhibitory concentration (IC<sub>50</sub>) was 39.19, 26.17 and 103.3 µg/mL for *P. ostreatus*, *L. edodes* and *A. bisporus*, respectively.

### Molecular Docking of Small Molecules

The 2D-Diagram of the docking study revealed that all the extracted compounds gave a C-DOCKER interaction energy in the range of 22.8–37.61 (Kcal/mol) with protease compared to boceprevir ligand of 41.6 (Kcal/mol). With similar binding mode with the essential amino acids forming hydrogen acceptor with GLU166, HIS164 and Pi interaction with MET165, LEU141 and HIS41 compared to ligand [Table 1](#). Catechin formed a more stable complex with protease binding site.

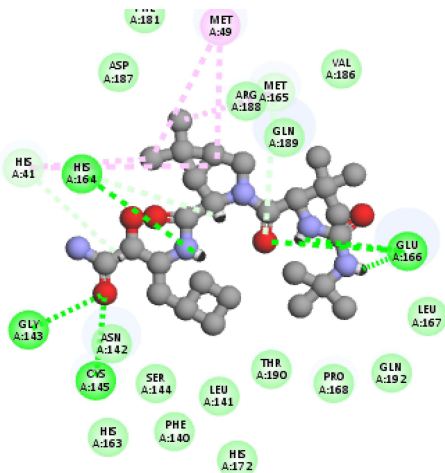
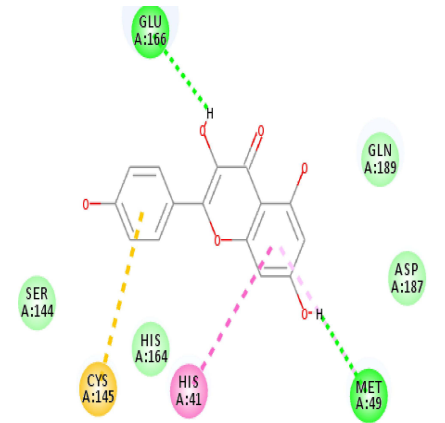
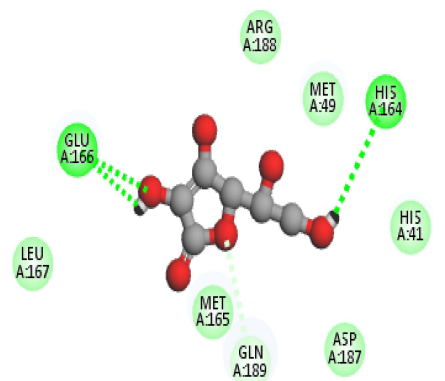
### Molecular Docking of Macromolecules

Results of the ZDOCK were visualized where top poses of the largest clusters were browsed and analyze protein interface was performed for interaction analysis of all the extracted proteins. Results showed that *A. bisporus* mushroom tyrosinase (PDB ID: 2Y9X) showed best interaction with protease target. *P. ostreatus* mushroom superoxide dismutase 1B06 and catalase 1DGG showed best interaction with protease target. [Figures 2–4](#) represents best z-ranked pose in best clustering (Pose 1, cluster 1) of 2Y9X, 1B06 and 1DGG, respectively with the M<sup>PRO</sup> protein 6XQU. [Tables 2–4](#)



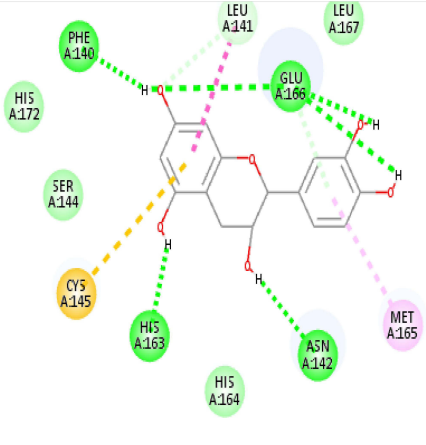
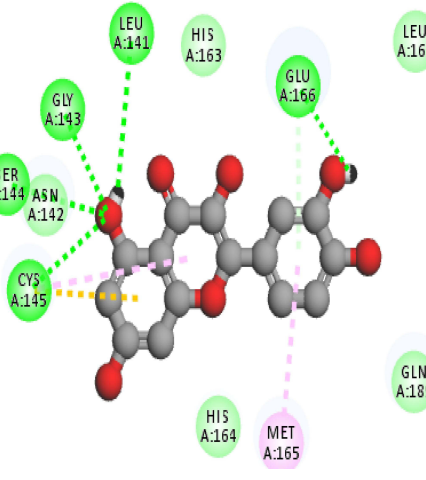
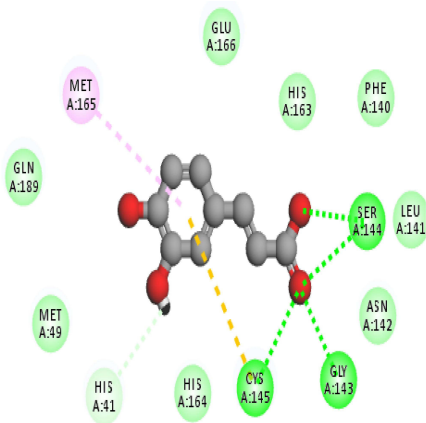
**Figure 1** Cytotoxicity concentration 50 (CC<sub>50</sub>) and infectivity concentration 50(IC<sub>50</sub>) of the three mushrooms *P. ostreatus*, *L. edodes* and *A. bisporus*.

**Table 1** The CDOKER Interaction Energy of the Small Molecule Ligands

Name	Binding Mode	-CDOKER Interaction Energy (kcal/mol)	Key Amino Acids Interaction
Boceprevir (Lead)		41.6	IHBA and IHBD with GLU166 IHBD with HIS164 I HBA with GLY143 I HBA with CYS145 Pi-alkyl with MET49 Pi-alkyl with HIS41
Kaempferol ( <i>P. ostreatus</i> )		36.5	2 HBD with GLU166 and MET49 Pi-alkyl with HIS41 Ring aromatic with CYS145
Ascorbic acid ( <i>Postreatus</i> , <i>L. edodes</i> , <i>A. bisporus</i> )		22.8	I HBA and IHBD with GLU166 IHBD with HIS164

(Continued)

Table I (Continued).

Name	Binding Mode	-CDOCKER Interaction Energy (kcal/mol)	Key Amino Acids Interaction
Catechin ( <i>P. ostreatus</i> , <i>L. edodes</i> and <i>A. bisporus</i> )		37.61	2 HBA and 1HBA with GLU166 1HBD with ASN142 1HBD with HIS163 1HBD with PHE140 Pi-alkyl with MET165 and LEU141
Quercetin ( <i>L. edodes</i> )		39.66	2HBAwith GLU166 1HBAwith GLY143 1HBAwith CYS145 Pi-alkyl MET49
Cholorgenic acid ( <i>A. bisporus</i> )		24.9	1 HBA with GLY143 1 HBA with CYS145 Pi-alkyl with MET165

**Abbreviations:** HB, Hydrogen Bond; HIS, Histidine; Leu, Leucine; GLU, Glutamic acid; GLY, Glycine; LEU, Leucine; MET, Methionine; CYS, Cysteine.



**Figure 2** Top pose in largest z-ranked clustering of mushroom tyrosinase (ribbon shaped) (2Y9X) from *A. bisporus* with MPR of COVID-19 (6XQU) (line shaped).

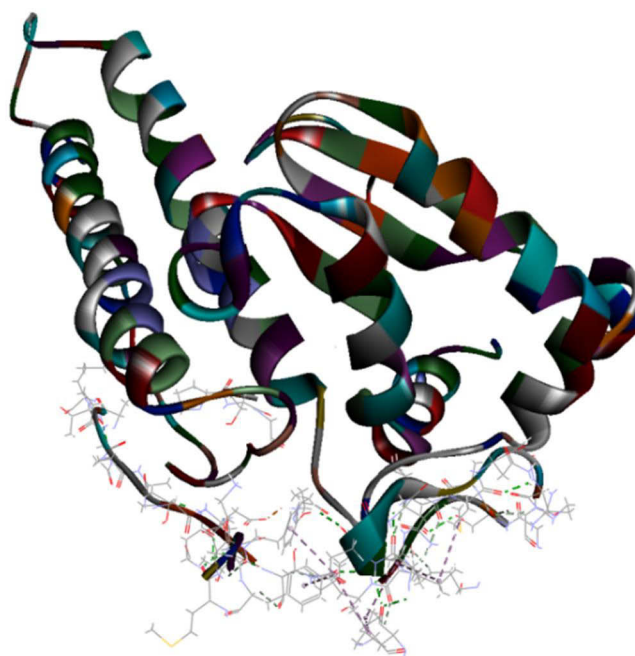


**Figure 3** Top pose in largest z-ranked clustering of superoxide dismutase (ribbon shaped) (1BO6) from *P. ostreatus*, *L. edodes* and *A. bisporus* with MPR of COVID-19 (6XQU) (line shaped).

4, showed 15 and 26 hydrogen bond interactions and 1 electrostatic interaction between amino acids chain in target and in ligand residues with 6XQU, respectively.

The Ligand Contact Surface Area with the protein was  $252.74 \text{ \AA}^2$  while Receptor Contact Surface Area was  $267.23 \text{ \AA}^2$ , which confirms good, and predicted Protein-Protein interaction. However, results showed no interaction of ubiquitin-



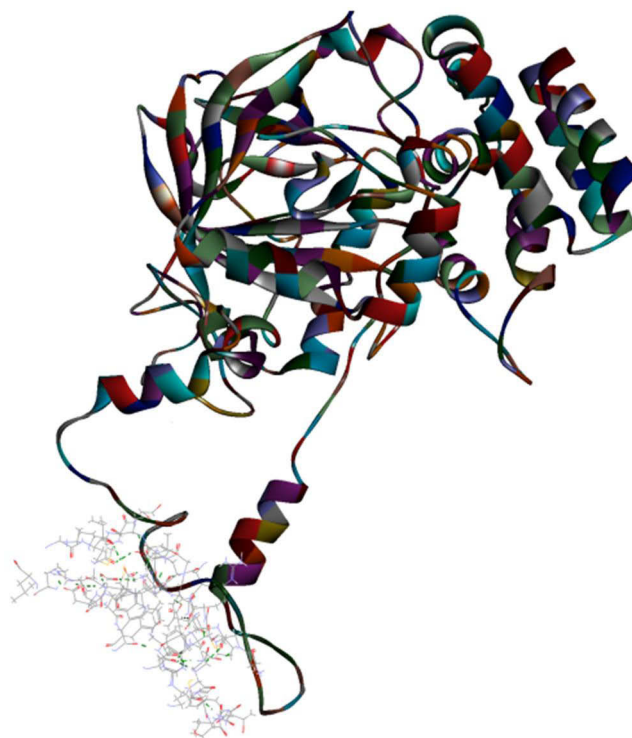


**Figure 4** Top pose in largest z-ranked clustering of catalase (IDGG) from *P. ostreatus*, *L. edodes* and *A. bisporus* with M<sup>pro</sup> of COVID-19 (6XQU) (line shaped).

like protein such as Rub1 (PDB ID: 1BT0) and valosin (PDB ID: 2X8A). [Figure 5A](#) and [B](#). ZDOCK results showed Z score and Z Rank of the different protein ligands and explained the different interaction of the different ligand proteins to the target. Where 2Y9X showed the highest results and 1BT0 showed the lowest results [Table 5](#).

## Molecular Dynamics Simulation

In the presented MD simulation, the best small molecule Catechin and the most promising macromolecule mushroom tyrosinase (PDB ID: 2Y9X) were subjected to MD simulation study to determine their dynamic properties and confirm the docking results. Screenshot samples of the uncropped results are depicted in the supplementary material for further review ([Figure S4](#), [Supplementary File](#)). Total energy versus time dynamics Plots of the docked ligand catechin was presented and compared to that of free 6XQU and undocked catechin. Also, the best macromolecule 2Y9X total energy versus time dynamics Plot was presented in [Figure 6](#). Where the docked catechin results showed stability after docking by  $-31.35$  and  $-31.45$  kcal/mol at time intervals 22 and 24, respectively. Compared to free undocked energy of 7.400, 7.550 kcal/mol and  $-1712$ ,  $-1413$  kcal/mol for catechin and 6XQU at time intervals 22 and 24, respectively. While 2Y9X showed  $-12,720$  and  $-12,730$  at time intervals 22 and 24, respectively ([Figure 6](#)). RMSD results of 6XQU before and after docking showed great similarity over the five different conformations. While RMSF versus Residue Index results indicated the stability of the complex at the binding site showing stability of 6QXU complex after docking with catechin (14.0) compared to the free 6XQU before docking (22.5). While 2Y9X showed comparable RMSD results with RMSF value of (3.5) showing good stability results ([Figure 7](#)).

## Discussion

In the current circumstances, with a pandemic that appears to be incurable and candidate medications still in the testing stage, other prophylactic and therapeutic principles must be considered. COVID-19 impose a life-threatening hazard to public health, in the light of absence of clinically approved therapy.<sup>26</sup> Furthermore, currently used treatment protocols are too expensive, sometimes unavailable; therefore, low-cost alternatives are urgently required. One potential candidate is

**Table 2** Main H-Bond & Electrostatic Interactions Between Mushroom Tyrosinase (2Y9X) and M<sup>Pro</sup> of COVID-19 (6XQU) Using ZDOCK Algorithm

Nr.	H-Bond Interaction
1	GLN107 - PRO274 Distance:2.56835
2	ASP155- GLU211 Distance:2.81658
3	PHE294 - PRO270 Distance:2.66147
4	GLY223 - SER301 Distance:2.79802
5	LYS102 - ASP203 Distance: 2.379
6	VAL104 - GLN205 Distance: 2.7794
7	GLY109 - ASP273 Distance: 2.0458
8	GLN110 - THR271 Distance: 2.61949
9	PRO252 - THR261 Distance: 2.33055
10	ALA260 - GLY249 Distance: 1.85874
11	ALA219 - GLY302 Distance: 1.91454
12	PRO222- SER301 Distance: 2.28743
13	GLY249 - SER254 Distance: 1.88965
	Electrostatic Interaction
1	LYS102 - ASP203 Distance: 1.63186

**Abbreviations:** HB, Hydrogen Bond; HIS, Histidine; Leu, Leucine; LYS, Lysine; GLU, Glutamic acid; GLN, Glutamine; GLY, Glycine; ASN, Asparagine; MET, Methionine; A, Alanine; ARG, Arginine; ASP, Aspartic acid; THR, Threonine; TYR, Tyrosine; SER, Serine.

prophylaxis and/or therapy using the medicinal mushrooms since they are rich in various biologically active metabolites and at lower cost.<sup>30</sup>

The Agaricomycotina among the Basidiomycetes mushrooms, *P. ostreatus* is a well-known medicinal mushroom that has been used worldwide for a range of diseases in traditional medicine.<sup>31</sup> The biologically active metabolites obtained from mushrooms have been proved to have potential antiviral activities.<sup>32</sup> It was previously reported that mushroom compounds diminish viral infection by several mechanisms.<sup>9</sup> They are rich in Bioactive compounds with potential antiviral activities including, polysaccharides, carbohydrate-binding proteins, peptides, enzymes (laccase and tyrosinase), several other compounds.<sup>33</sup> It was previously confirmed that mushrooms can suppress viral entry, replication, in addition to their interfering properties in the protein expression.<sup>8</sup> It was previously reported that certain mushroom proteins can enhance immunity against many viruses particularly those of relevant medical importance.<sup>8</sup> Interestingly, polysaccharide, lectin, lentin, and laccase from certain mushrooms showed IC<sub>50</sub> in the range of 0.1–2.2 µM against HIV-1.<sup>34,35</sup>

The current study investigated the antiviral activity of *P. ostreatus*, and *L. edodes* showed a promising cytotoxic activity against COVID –19 with IC<sub>50</sub> 39.19 µg/mL and 26.17 µg/mL, respectively. However, *A. bisporus* showed a moderate activity with IC<sub>50</sub> 103.3 µg/mL. Evaluation of the antiviral related activity to the biologically active chemicals was evidenced by in silico molecular modeling. Three small molecules; catechin, kaempferol and ascorbic acid, were found to bind to the M<sup>Pro</sup> of SARS-CoV-2 which is essential for viral replication. Another highly bioactive catechin, Epigallocatechin gallate (EGCG) is known to prevent influenza A and B virus infections in Madin-Darby canine kidney cells.<sup>36</sup> Furushima et al also reported that tea catechins repressed influenza viral infections by many

**Table 3** Main H-Bond Interactions Between Superoxide Dismutase (IBO6) and M<sup>Pro</sup> of COVID-19 (6XQU)

Nr.	H-Bond Interaction
1	LYS5 - GLU288, Distance: 2.42393
2	ASN133-ASN133, Distance:2.41124
3	ASN133 - GLY195, Distance:1.86636
4	GLN192 - THR190, Distance:2.44148
5	THR199 - ASN238, Distance:1.96504
6	TYR237 - LEU272, Distance:2.575
7	ASN238 - MET235, Distance:2.1777
8	ASN238 - ASP197, Distance:1.89557
9	LEU271 - LEU268, Distance:2.17933
10	LEU272 - LEU268, Distance:2.01215
11	ASN274- LEU271, Distance:2.7241
12	GLY275 - LEU271, Distance:2.08039
13	ARG279 - MET276, Distance:2.37018
14	SER284 - LEU286, Distance:2.35955
15	ASP289-A:ASP289, Distance:2.5352

**Abbreviations:** HB, Hydrogen Bond; HIS, Histidine; Leu, Leucine; LYS, Lysine; GLU, Glutamic acid; GLN, Glutamine; GLY, Glycine; ASN, Asparagine; MET, Methionine; A, Alanine; ARG, Arginine; ASP, Aspartic acid; THR, Threonine; TYR, Tyrosine; SER, Serine.

**Table 4** Main H-Bond Interactions Between Catalase (1DGG) and M<sup>Pro</sup> of COVID-19 (6XQU)

Nr.	H-Bond Interaction	Nr.	H-Bond Interaction
1	GLY2 - ASN214, Distance:1.8821	14	ASN214 - ALA210, Distance:2.06651
2	ARG4 - GLN299, Distance:1.72967	15	ASN214 - ALA211, Distance:2.34427
3	LYS5:HZ1 -GLU288, Distance:2.42393	16	ASN214 - ALA210, Distance:2.02583
4	LYS5:HZ2 - GLU290, Distance:2.44722	17	ASN214- GLY2, Distance:2.9962
5	MET6 - ARG4, Distance:3.04741	18	ASP216 - ALA211, Distance:1.82505
6	VAL114 - TYR126, Distance:1.78011	19	ILE281 - SER284, Distance:1.79437
7	TYR126 - VAL114, Distance:2.10321	20	LEU282- ASP216, Distance:2.12104
8	CYS128 - LYS137, Distance:2.33231	21	SER284 - ILE281, Distance:1.86869
9	ALA129 - GLU290; Distance:2.70004	22	SER284 - LEU286, Distance:2.35955
10	ARG131 - ASP289, Distance:1.77286	23	ASP289 - ASP289, Distance:2.5352
11	ARG131 - ASP289, Distance:1.7424	24	GLN299 - ARG4, Distance:1.79192
12	SER139:HN - TYR126, Distance:1.96164	25	GLY302 - ARG298, Distance:2.08336
13	ALA211 - TRP207, Distance:1.8078	26	VAL303- ARG298, Distance:2.32314

**Abbreviations:** HB, Hydrogen Bond; HIS, Histidine; Leu, Leucine; LYS, Lysine; GLU, Glutamic acid; GLN, Glutamine; GLY, Glycine; ASN, Asparagine; MET, Methionine; A, Alanine; ARG, Arginine; ASP, Aspartic acid; THR, Threonine; TYR, Tyrosine; SER, Serine; CYS, Cysteine; VAL, Valine.

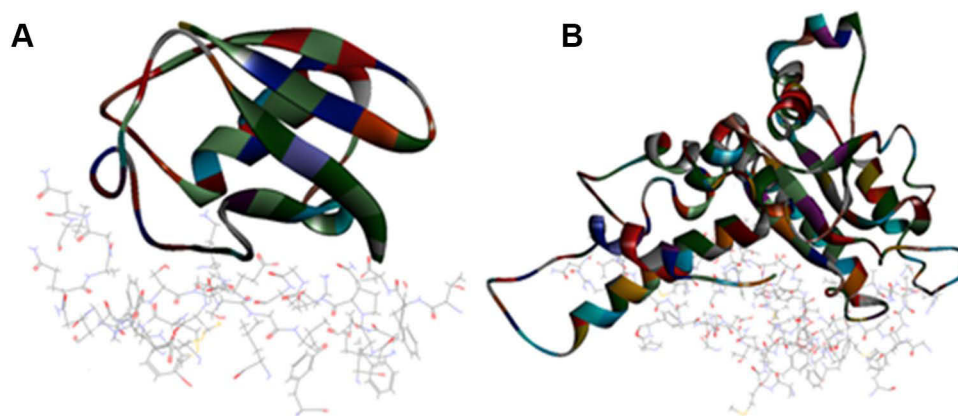


**Figure 5** Top pose in largest z-ranked clustering of (A) Ubiquitin like protein (ribbon shaped) (IBT0) from *P. ostreatus*, *L. edodes* and *A. bisporus*. (B) Valosin (2X8A) from *L. edodes* with M<sup>pro</sup> of COVID-19 (6XQU) (line shaped).

mechanisms.<sup>31</sup> It was also previously documented, that catechins showed promising activities against some cold viruses<sup>31</sup> as well as immunomodulatory activities against viral infection.<sup>36</sup>

Kaempferol was also found to interact with the binding site M<sup>pro</sup> of SARS-CoV-2. Huang et al 2020<sup>34</sup> also reported the anti-SARS-CoV-2 activity of kaempferol based on the inactivation of protein kinase B, phosphorylation of protein kinase and blocking the 3a channel in SARS-CoV infected cells. In addition to, its anti-inflammatory and immunomodulatory effects.<sup>37</sup>

As it was reported in our findings that ascorbic acid was the only vitamin found in high amount relative to other vitamins in the mushroom extract.<sup>36</sup> There is a prove that ascorbic acid and quercetin co-administration employs a synergistic antiviral activity.<sup>32</sup> The use of vitamin C and quercetin combination was recently reported for prophylaxis and management of COVID-19 patients in addition to remdesivir or convalescent plasma.<sup>38</sup> During infection, vitamin C is concentrated within macrophages, is essential for neutrophil killing, is responsible for T cell maturation, in addition to promoting phagocytosis and apoptosis of spent neutrophils.<sup>39</sup>

The obtained molecular docking result revealed that SARS-CoV-2 M<sup>pro</sup> is considered a key enzyme with a vital role in viral replication. This makes it an appealing target for drug invention of new COVID-19 candidates. The extracted compounds from mushroom showed antiviral activity with promising anti COVID results after molecular simulation study via docking on 6XQU. C-DOCKER protocol was applied on small molecules while ZDOCK was used for protein-protein docking on the extracted proteins. The findings indicated the highest binding interaction for quercetin on protease with (E= -39.66 Kcal/mol) showing interaction with the key amino acids via 2 HBA with GLU166, and 1 HBA with each of GLY143 & CYS145. In addition to Pi-alkyl interaction with MET165 compared to ligand (E= -41.6 Kcal/mol). While catechin (E= -37.61 Kcal/mol) showed an additional HBA interaction with GLU166 compared to ligand and an additional Pi-alkyl interaction with MET165 compared to ligand. Caffeic acid (E= -24.9 Kcal/mol) showed 1 HBA with GLY143 & CYS145 and an additional Pi-alkyl interaction with MET165. Ascorbic acid (E= -22.8 Kcal/mol)

**Table 5** ZDOCK Results for the Different Ligand Proteins

Ligand Protein	Z Score	Z Rank (kcal/mol)
2Y9X (Tyrosinase, <i>A. bisporus</i> )	19.75	-121.32
2X8A (Valosin, <i>L. edodes</i> )	18.78	-115.80
IBO6 (Superoxidase dismutase, <i>P. ostreatus</i> , <i>L. edodes</i> and <i>A. bisporus</i> )	18.46	-117.84
IDGG (Catalase, <i>P. ostreatus</i> , <i>L. edodes</i> and <i>A. bisporus</i> )	17.94	-130.59
IBT0 (Ubiquitin, <i>P. ostreatus</i> , <i>L. edodes</i> and <i>A. bisporus</i> )	14.72	-84.7

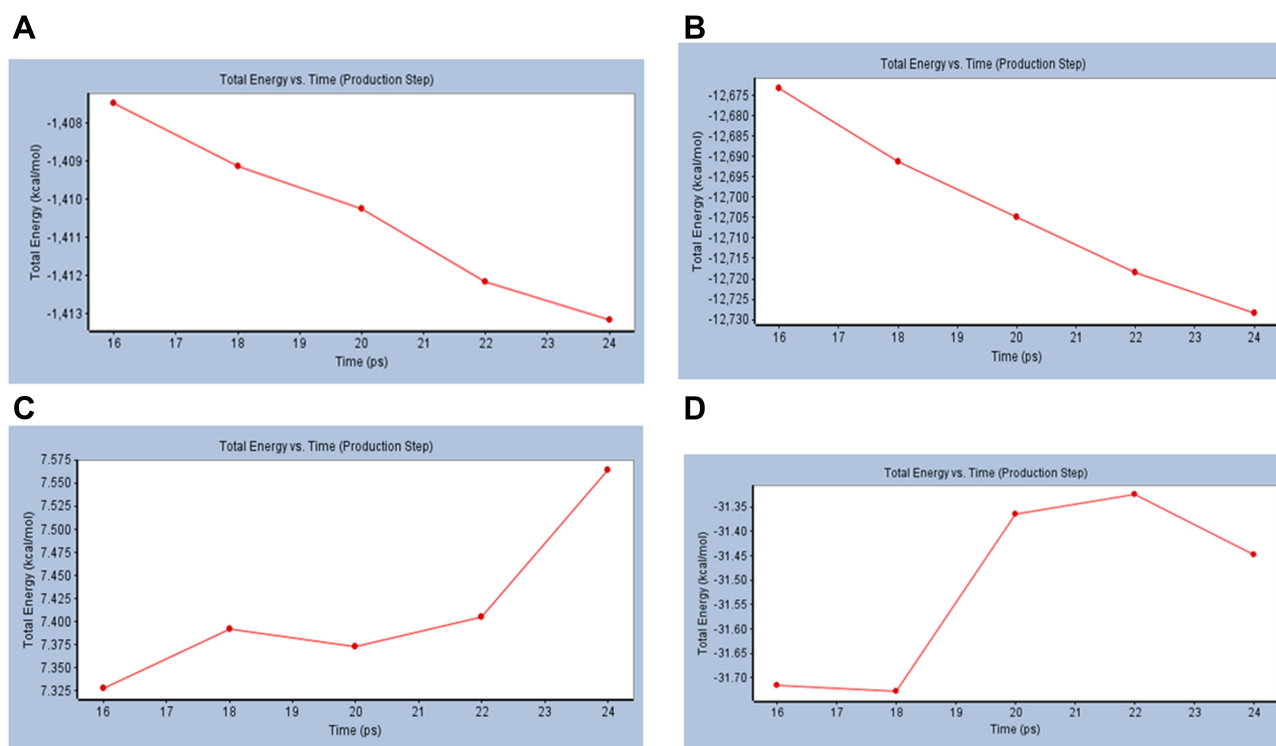


**Figure 6** Total energy versus time dynamics plot for (A) M<sup>pro</sup> of COVID-19 (6XQU), (B) Mushroom tyrosinase (2Y9X), (C) undocked catechin and (D) Catechin complexed with 6XQU after docking.

showed 2 HBA with GLU166 and 1HBA with HIS164. Other studies reported that aqueous solvent was employed to prepare raw extracts of *V. vinifera* leaves and its chemical profile was analyzed through HPLC-MS in negative ionization mode. This analysis led to the identification of 35 flavonoids, most of which were derivatives of quercetin. Others included derivatives of luteolin, kaempferol, apigenin, isorhamnetin, myricetin, chrysoeriol, biochanin, isookanin, and scutellarein. Furthermore, the antiviral potential of the extract was tested against HSV-1 and SARS-CoV-2 with very interesting results, showing the capability of flavonoids to inhibit SARS-CoV-2 for the first time. Considering the current pandemic emergency, our results represent a promising resource for pharmaceutical industrial applications.

ZDOCK algorithm was used to predict protein-protein interaction between the extracted proteins and 6XQU. The “Analyze Protein Interface” Report from discovery studio after ZDOCK showed that Ligand Contact Surface Area with the protein as 252.74 Å<sup>2</sup> while Receptor Contact Surface Area was 267.23 Å<sup>2</sup>. These results confirmed good interaction between the target protease protein and the docked ligand protein. Result visualization indicated that mushroom tyrosinase (2Y9X) revealed the best interaction via hydrogen bonding with the essential amino acids in the binding site (Z Rank= -121.32 kcal/mol). The interaction showed 13 hydrogen bonds and 1 electrostatic interaction between amino acids chain in target and in Ligand residues. While valosin (2X8A) and ubiquitin-like protein, Rub1 (1BT0) showed no binding interaction with protease interface (Z Rank= -115.80, -84.7 kcal/mol, respectively). On the other hand, catalase (PDB ID: 1DGG) and superoxide dismutase (PDB ID: 1BO6) showed good binding interaction at the protein interface (Z Rank= -130.59, -117.84 kcal/mol, respectively). MD simulation study on the two most promising docked ligands (catechin and 2Y9X) showed that low free binding energy versus time results after ligand binding to 6XQU confirming stable docked complexes with the target 6XQU compared to the free undocked form. Generally, RMSD calculates the deviation extent to the respective reference structure. Hereby, the low RMSD values are correlated to significant stability, relative to the conformation of the docked molecule. So, ligands with low RMSD values, in their respective ligand–protein complex, would reveal good ligand fitting within the targeted pocket via the adopted MD simulation time-frames.<sup>29</sup> RMSF results versus residue index showed good stability of the complexed binding site.

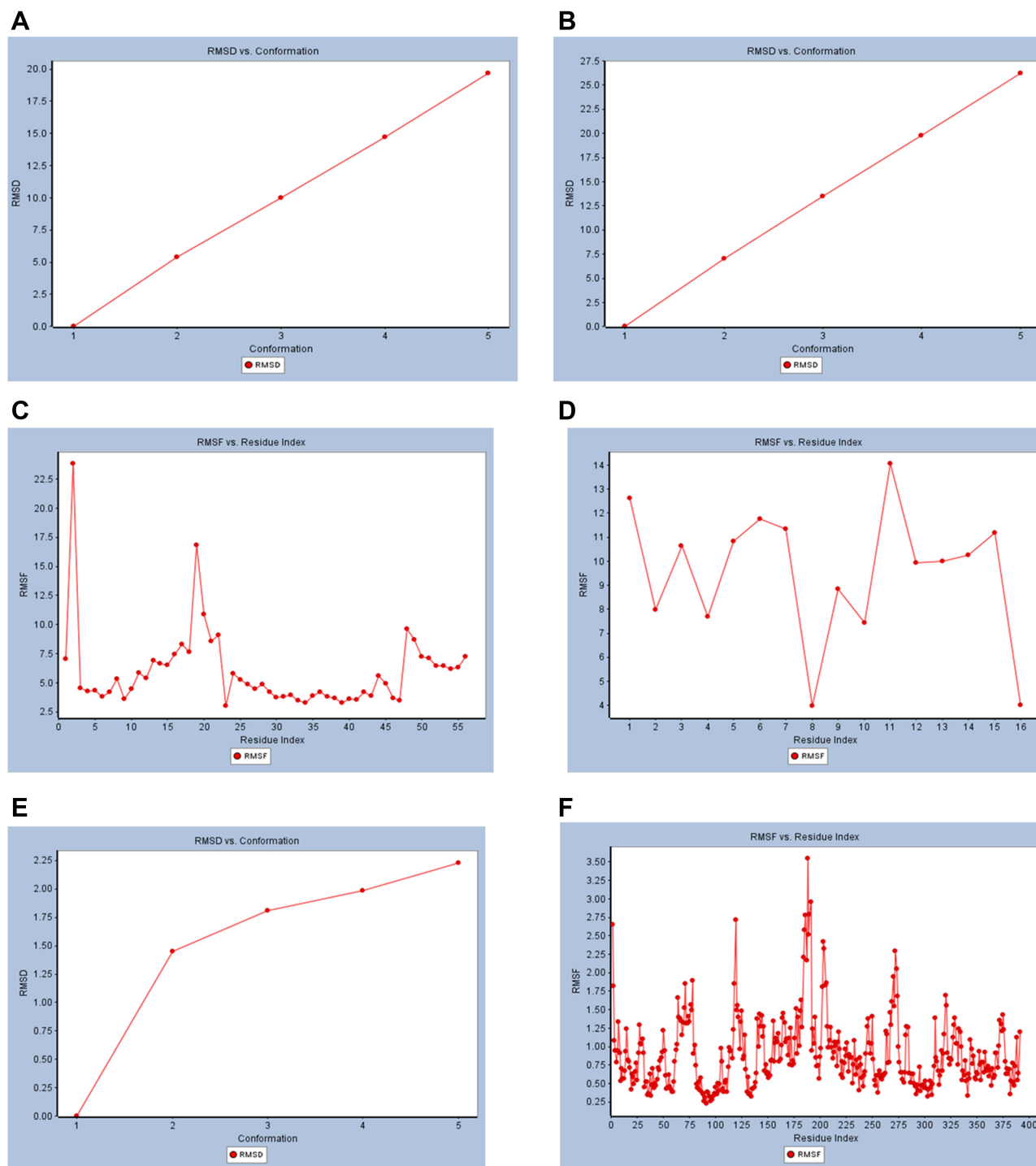


**Figure 7** Dynamic simulation of (A) RMSD plot of  $M^{Pro}$  of COVID-19 (6XQU) before docking, (B) RMSD plot of (6XQU) after catechin docking, (C) RMSF plot of 6XQU before docking, (D) RMSF plot of 6XQU after catechin docking, (E) RMSD plot of mushroom tyrosinase (2Y9X), and (F) RMSF plot of mushroom tyrosinase (2Y9X).

Where it defines the fluctuations contributed to protein individual residues with the ligand/protein complex. RMSF evaluates the time evolution of the mean deviation for every residue relative to its reference position.

Complement Drugs or compounds with special properties on viral protease inhibitors have been believed as potential medications against CoVs.<sup>40–42</sup> It was previously reported that, the viral proteases can identify the specific sequences of

amino acids in their targets and split the peptide bond.<sup>41,42</sup> Fungal metabolites potential activities as protease inhibitors have gained the attention of many recent studies.<sup>22–24</sup> In our study, the effects of the extracted edible mushrooms on COVID-19 were conducted in vitro using Vero-E6 cells followed by molecular docking analysis of different small molecules using CDOKER and macromolecules using ZDOCK protocol against M<sup>Pro</sup> of COVID-19.

## Conclusion

Aqueous extracts of *P. ostreatus*, *L. edodes* and *A. bisporus* showed in vitro antiviral activities against SARS-CoV-2 with a high selectivity to the viral infected cells. Small fungal biomolecules including, quercetin from *L. edodes*, kaempferol from *P. ostreatus*, chlorogenic acid from *A. bisporus*, ascorbic acid and catechin of the three mushrooms extracts and macromolecules including, tyrosinase from *A. bisporus* and superoxide dismutase and catalase of the three fungal extracts were able to effectively bind to the M<sup>Pro</sup> of SARS-CoV-2 as indicated by in silico docking analysis. Further, in vivo investigations are recommended to estimate the antiviral activities of the respective active metabolites for the potential use in humans.

## Data Sharing Statement

All the data supporting the findings are included in the manuscript and [Supplementary File](#).

## Acknowledgments

The authors extend their gratitude to the Microbiology and Immunology Department, Faculty of Pharmacy, Ain Shams University, and Ahram Canadian University (ACU) Cairo, Egypt, for the great help and support in the current study. The authors are grateful for Dr. Asmaa A Mandour, Pharmaceutical Chemistry Department, Faculty of Pharmacy, Future University in Egypt (FUE), Cairo, 11835, Egypt, for docking analysis. The authors express their appreciation to the Deanship of Scientific Research at King Khalid University for funding this work through the research groups program under grant number R.G.P.2/111/41. The authors extend their appreciation to the Deputyship for Research & Innovation, Ministry of Education, in Saudi Arabia, for funding this research work through the project number: IFP-KKU-2020/10.

## Disclosure

The authors declare that they have no conflicts of interest in relation to this work.

## References

1. Cauchemez S, Van Kerkhove MD, Riley S, Donnelly CA, Fraser C, Ferguson NM. Transmission scenarios for middle east respiratory syndrome coronavirus (MERS-CoV) and how to tell them apart. *Euro Surveill*. 2013;18(24):20503. doi:10.2807/ese.18.24.20503-en
2. Cui J, Shen HM, Lim LHK. The role of autophagy in liver cancer: crosstalk in signaling pathways and potential therapeutic targets. *Pharmaceuticals*. 2020;13(12):432. doi:10.3390/ph13120432
3. Zhu N, Zhang D, Wang W, et al. A novel coronavirus from patients with pneumonia in China, 2019. *N Engl J Med*. 2020;382(8):727–733. doi:10.1056/NEJMoa2001017
4. Li Q, Guan X, Wu P, et al. Early transmission dynamics in Wuhan, China, of novel coronavirus-infected pneumonia. *N Engl J Med*. 2020;382(13):1199–1207. doi:10.1056/NEJMoa2001316
5. Xu J, Zhao S, Teng T, et al. Systematic comparison of two animal-to-human transmitted human coronaviruses: SARS-CoV-2 and SARS-CoV. *Viruses*. 2020;12(2):244. doi:10.3390/v12020244
6. Lim J, Jeon S, Shin HY, et al. The author's response: case of the index patient who caused tertiary transmission of coronavirus disease 2019 in Korea: the application of lopinavir/ritonavir for the treatment of COVID-19 pneumonia monitored by quantitative RT-PCR. *J Korean Med Sci*. 2020;35(7):e89. doi:10.3346/jkms.2020.35.e89
7. Stebbing J, Phelan A, Griffin I, et al. COVID-19: combining antiviral and anti-inflammatory treatments. *Lancet Infect Dis*. 2020;20(4):400–402. doi:10.1016/S1473-3099(20)
8. Lin LT, Hsu WC, Lin CC. Antiviral natural products and herbal medicines. *J Tradit Complement Med*. 2014;4(1):24–35. doi:10.4103/2225-4110.124335
9. Akram M, Tahir IM, Shah SMA, et al. Antiviral potential of medicinal plants against HIV, HSV, influenza, hepatitis, and coxsackievirus: a systematic review. *Phytother Res*. 2018;32(5):811–822. doi:10.1002/ptr.6024
10. Bellettini MB, Fiorda FA, Maievas HA, et al. Factors affecting mushroom *Pleurotus* spp. *Saudi J Biol Sci*. 2019;26(4):633–646. doi:10.1016/j.sjbs.2016.12.005
11. Cardwell G, Bornman JF, James AP, Black LJ. A review of mushrooms as a potential source of dietary vitamin D. *Nutrients*. 2018;10:10. doi:10.3390/nu10101498

12. Koutrotsios G, Tagkouli D, Bekiaris G, et al. Enhancing the nutritional and functional properties of *Pleurotus citrinopileatus* mushrooms through the exploitation of winery and olive mill wastes. *Food Chem.* 2022;370:131022. doi:10.1016/j.foodchem.2021.131022
13. Tsiatas K, Tsiaka T, Koutrotsios G, et al. On the identification and quantification of ergothioneine and lovastatin in various mushroom species: assets and challenges of different analytical approaches. *Molecules.* 2021;26(7):1832. doi:10.3390/molecules26071832
14. Lo YC, Lin SY, Ulzijargal E, et al. Comparative study of contents of several bioactive components in fruiting bodies and mycelia of culinary-medicinal mushrooms. *Int J Med Mushrooms.* 2012;14(4):357–363. doi:10.1615/intjmedmushr.v14.i4.30
15. Lindequist U, Niedermeyer THJ, Jülich WD. The pharmacological potential of mushrooms. *Evid Based Complement Alternat Med.* 2005;2(3):285–299. doi:10.1093/ecam/neh107
16. Majtan J. Pleuran ( $\beta$ -glucan from *Pleurotus ostreatus*): an effective nutritional supplement against upper respiratory tract infections? *Med Sport Sci.* 2012;59:57–61. doi:10.1159/000341967
17. Ren G, Xu L, Lu T, Yin J. Structural characterization and antiviral activity of lentinan from *Lentinus edodes* mycelia against infectious hematopoietic necrosis virus. *Int J Biol Macromol.* 2018;115:1202–1210. doi:10.1016/j.ijbiomac.2018.04.132
18. Rop O, Mlecek J, Jurikova T. Beta-glucans in higher fungi and their health effects. *Nutr Rev.* 2009;67(11):624–631. doi:10.1111/j.1753-4887.2009.00230.x
19. McCarty MF, DiNicolantonio JJ. Nutraceuticals have potential for boosting the type 1 interferon response to RNA viruses including influenza and coronavirus. *Prog Cardiovasc Dis.* 2020;63(3):383–385. doi:10.1016/j.pcad.2020.02.007
20. Elhusseiny SM, El-Mahdy TS, Awad MF, et al. Proteome Analysis and in vitro antiviral, anticancer and antioxidant capacities of the aqueous extracts of *Lentinula edodes* and *Pleurotus ostreatus* edible mushrooms. *Molecules.* 2021;26(15):4623. doi:10.3390/molecules26154623
21. Mostafa A, Kandeil A, Elshaier Y AMM, et al. FDA-approved drugs with potent in vitro antiviral activity against severe acute respiratory syndrome coronavirus 2. *Pharmaceuticals.* 2020;13(12):443. doi:10.3390/ph13120443
22. Krupodorova T, Rybalko S, Barshteyn V. Antiviral activity of Basidiomycete mycelia against influenza type A (serotype H1N1) and herpes simplex virus type 2 in cell culture. *Virol Sin.* 2014;29(5):284–290. doi:10.1007/s12250-014-3486-y
23. Hetland G, Johnson E, Bernardshaw SV, Grinde B. Can medicinal mushrooms have prophylactic or therapeutic effect against COVID-19 and its pneumonic superinfection and complicating inflammation? *Scand J Immunol.* 2021;93(1):e12937. doi:10.1111/sji.12937
24. Facchini JM, Alves EP, Aguilera C, et al. Antitumor activity of *Pleurotus ostreatus* polysaccharide fractions on Ehrlich tumor and sarcoma 180. *Int J Biol Macromol.* 2014;68:72–77. doi:10.1016/j.ijbiomac.2014.04.033
25. Seo D, Choi C. Antiviral bioactive compounds of mushrooms and their antiviral mechanisms: a review. *Viruses.* 2021;13:350. doi:10.3390/v13020350
26. Li X, Wang Z, Wang L, Walid E, Zhang H. In vitro antioxidant and anti-proliferation activities of polysaccharides from various extracts of different mushrooms. *Int J Mol Sci.* 2012;13(5):5801–5817. doi:10.3390/ijms13055801
27. Borgia JF, Alsuwat HS, Al Otaibi WM, et al. State-of-The-art tools unveil potent drug targets amongst clinically approved drugs to inhibit helicase in SARS-CoV-2. *Arch Med Sci.* 2020;16(3):508. doi:10.5114/aoms.2020.94567
28. Azeez SA, Alhashim ZG, Al Otaibi WM, et al. State-of-The-art tools to identify druggable protein ligand of SARS-CoV-2. *Arch Med Sci.* 2020;16(3):497. doi:10.5114/aoms.2020.94046
29. Al-Karmalawy AA, Dahab MA, Metwaly AM, et al. Molecular docking and dynamics simulation revealed the potential inhibitory activity of ACEIs against SARS-CoV-2 targeting the hACE2 receptor. *Front Chem.* 2021;9. doi:10.3389/fchem.2021.661230
30. Wang HX, Ng TB. Isolation of a novel ubiquitin-like protein from *Pleurotus ostreatus* mushroom with anti-human immunodeficiency virus, translation-inhibitory, and ribonuclease activities. *Biochem Biophys Res Commun.* 2000;276(2):587–593. doi:10.1006/bbrc.2000.3540
31. Furushima D, Ide K, Yamada H. Effect of tea catechins on influenza infection and the common cold with a focus on epidemiological/clinical studies. *Molecules.* 2018;23(7):1795. doi:10.3390/molecules23071795
32. Huang YF, Bai C, He F, Xie Y, Zhou H. Review on the potential action mechanisms of Chinese medicines in treating coronavirus disease 2019 (COVID-19). *Pharmacol Res.* 2020;158:104939. doi:10.1016/j.phrs.2020.104939
33. Colunga Biancatelli RML, Berrill M, Catravas JD, Marik PE. Quercetin and vitamin c: an experimental, synergistic therapy for the prevention and treatment of SARS-CoV-2 related disease (COVID-19). *Front Immunol.* 2020;11:1451. doi:10.3389/fimmu.2020.01451
34. Anderson O, Beckett J, Briggs CC, et al. An investigation of the antileishmanial properties of semi-synthetic saponins. *RSC Med Chem.* 2020;11(7):833–842. doi:10.1039/d0md00123f
35. Puente XS, Sánchez LM, Overall CM, López-Otín C. Human and mouse proteases: a comparative genomic approach. *Nat Rev Genet.* 2003;4(7):544–558. doi:10.1038/nrg1111
36. Drag M, Salvesen GS. Emerging principles in protease-based drug discovery. *Nat Rev Drug Discov.* 2010;9(9):690–701. doi:10.1038/nrd3053
37. Kumar S, Stecher G, Li M, Knyaz C, Tamura K. MEGA X: molecular evolutionary genetics analysis across computing platforms. *Mol Biol Evol.* 2018;35(6):1547–1549. doi:10.1093/molbev/msy096
38. Giunco AJ, Paz MFD, Fonseca GG. Development and evaluation of low-carb cakes produced from green bocaiuva pulp enriched with *Pleurotus ostreatus*. *J Culinary Sci Technol.* 2021;1–13. doi:10.1080/15428052.2021.1929637
39. Barbosa JR, Freitas MM, Oliveira LC, et al. Obtaining extracts rich in antioxidant polysaccharides from the edible mushroom *Pleurotus ostreatus* using binary system with hot water and supercritical CO<sub>2</sub>. *Food Chem.* 2020;330:127173. doi:10.1016/j.foodchem.2020.127173
40. Singh A, Sharma S, Singh B. Influence of grain activation conditions on functional characteristics of brown rice flour. *Food Sci Technol Int.* 2017;23(6):500–512. doi:10.1177/1082013217704327
41. Duffy SK, Kelly AK, Rajauria G, et al. The use of synthetic and natural vitamin D sources in pig diets to improve meat quality and vitamin D content. *Meat Sci.* 2018;143:60–68. doi:10.1016/j.meatsci.2018.04.014
42. Rangsinth P, Sillapachaiyaporn C, Nilkhet S, Tencomnao T, Ung AT, Chuchawankul S. Mushroom-derived bioactive compounds potentially serve as the inhibitors of SARS-CoV-2 main protease: an in silico approach. *J Tradit Complement Med.* 2021;11(2):158–172. doi:10.1016/j.jtcm.2020.12.002



Infection and Drug Resistance

Dovepress

### Publish your work in this journal

Infection and Drug Resistance is an international, peer-reviewed open-access journal that focuses on the optimal treatment of infection (bacterial, fungal and viral) and the development and institution of preventive strategies to minimize the development and spread of resistance. The journal is specifically concerned with the epidemiology of antibiotic resistance and the mechanisms of resistance development and diffusion in both hospitals and the community. The manuscript management system is completely online and includes a very quick and fair peer-review system, which is all easy to use. Visit <http://www.dovepress.com/testimonials.php> to read real quotes from published authors.

Submit your manuscript here: <https://www.dovepress.com/infection-and-drug-resistance-journal>